Article

The Use of MgO Obtained from Serpentinite in the Synthesis of a Magnesium Potassium Phosphate Matrix for Radioactive Waste Immobilization

Svetlana A. Kulikova [1,*], Sergey E. Vinokurov [1], Ruslan K. Khamizov [1], Natal'ya S. Vlasovskikh [2], Kseniya Y. Belova [1], Rustam K. Dzhenloda [1], Magomet A. Konov [2] and Boris F. Myasoedov [1]

[1] Vernadsky Institute of Geochemistry and Analytical Chemistry, Russian Academy of Sciences, 19 Kosygin st., 119991 Moscow, Russia; vinokurov.geokhi@gmail.com (S.E.V.); khamiz@mail.ru (R.K.K.); ksysha_3350@mail.ru (K.Y.B.); dzhenloda@gmail.com (R.K.D.); bfmyas@mail.ru (B.F.M.)

[2] JSC Scientific Production Enterprise "Radiy", 28 Chasovaya st., 125315 Moscow, Russia; newchemtechnology@mail.ru (N.S.V.); info@npp-radiy.ru (M.A.K.)

* Correspondence: kulikova.sveta92@mail.ru; Tel.: +7-495-939-7007

Featured Application: MgO is used for the synthesis of a magnesium potassium phosphate matrix as a material for immobilization of radioactive waste in order to ensure radiation safety during storage or disposal of waste.

Abstract: Magnesium oxide is a necessary binding agent for the synthesis of a magnesium potassium phosphate (MPP) matrix based on $MgKPO_4 \times 6H_2O$, which is promising for the solidification of radioactive waste (RW) on an industrial scale. The performed research is devoted to finding a cost-effective approach to the synthesis of MPP matrix by using MgO with an optimal ratio of the quality of the binding agent and the cost of its production. A method for obtaining MgO from the widely available natural mineral serpentinite was proposed. The phase composition, particle morphology, and granulometric composition of MgO were studied. It was found that the obtained MgO sample, in addition to the target periclase phase, also contains impurities of brucite and hydromagnesite; however, after calcining at 1300 °C for 3 h, MgO transforms into a monophase state with a periclase structure with an average crystallite size of 62 nm. The aggregate size of the calcined MgO powder in an aqueous medium was about 55 μm (about 30 μm after ultrasonic dispersion), and the specific surface area was 5.4 m^2/g. This powder was used to prepare samples of the MPP matrix, the compressive strength of which was about 6 MPa. The high hydrolytic stability of the MPP matrix was shown: the differential leaching rate of magnesium, potassium, and phosphorus from the sample on the 91st day of its contact with water does not exceed 1.6×10^{-5}, 4.7×10^{-4} и8.9×10^{-5} g/(cm²·day), respectively. Thus, it was confirmed that the obtained MPP matrix possesses the necessary quality indicators for RW immobilization.

Keywords: serpentinite; magnesium oxide; calcination; particle size distribution; specific surface area; magnesium potassium phosphate matrix; radioactive waste; immobilization; hydrolytic stability; strength

1. Introduction

Industrial activities associated with the production and use of materials containing radioactive substances inevitably lead to the generation of radioactive waste (RW) of various activity levels. The largest amount of RW is generated during the operation of nuclear fuel cycle enterprises and exploitation of nuclear power reactors of various purposes. In some countries, including the USA, Sweden, and Finland, spent nuclear fuel (SNF) of nuclear power reactors is classified as RW and is stored without reprocessing. In other countries, including Russia, France, and Japan, SNF is subject to reprocessing for the purpose of

extraction of uranium and plutonium for reuse, as well as a number of valuable components from fission products and actinides, and the residue part is considered to be RW. In case of uncontrolled spread of radioactive substances, they have a negative impact on humans and environmental objects. Therefore, solving the problem of RW management in order to ensure their reliable isolation from the human environment is key for the further development of nuclear energy and industry. For controlled storage and/or final disposal of RW, it should be converted to a stable solidified form using stable matrices.

Earlier, we showed in [1–5] that magnesium potassium phosphate (MPP) matrix $MgKPO_4 \times 6H_2O$ is an effective and multipurpose mineral-like material for immobilization of different RW, and it possesses the number of benefits over cement and glass-like compounds. Therefore, MPP matrix was investigated for solidification of liquid intermediate level waste (ILW) [1], high level waste (HLW) [2,3], and also RW containing radiocarbon [14]C [4] and spent electrolyte [5], obtained as a result of pyrochemical reprocessing of mixed nitride uranium-plutonium SNF. This matrix is obtained by the acid-base reaction (1) of magnesium oxide (MgO) with potassium dihydrogen phosphate (KH_2PO_4) in an aqueous solution at room temperature, and it is an analog of the natural mineral K-struvite [6].

$$MgO + KH_2PO_4 + 5H_2O \rightarrow MgKPO_4 \times 6H_2O \qquad (1)$$

Magnesium oxide is a necessary binding agent for reaction (1) for the synthesis of MPP matrix; it is usually produced by calcination of carbonate minerals—magnesite ($MgCO_3$) [7] and dolomite ($CaMg(CO_3)_2$) [8]. It is widely used to obtain the refractories in the production of steel and cement (70–80% of world consumption) in electrical engineering, agriculture, for wastewater treatment, and gas absorption. Magnesium oxide on the market with a purity of at least 99 wt% has a high cost—up to $5000 per ton. At the same time, it is obvious that for the competitiveness of the technology of RW solidification using the MPP matrix, cheaper raw materials should be used; for example, so that the cost of MgO is at the level of the cost of Portland cement ($300–400 per ton). For this reason, the aim of the study was to find a cost-effective approach to synthesizing the MPP matrix through the use of MgO with low production cost. In this regard, a natural mineral, serpentinite ($Mg_3Si_2O_5(OH)_4$), which contains 32–38% of MgO [9], is of special interest. There are various technologies for reprocessing of serpentinite, primarily methods using mineral acids: sulfuric acid [10], nitric acid [9], and hydrochloric acid [11].

Earlier in [12], while testing several commercial MgO samples obtained from magnesite, we recommended the use of MgO powder with an average particle size of about 50 μm, which has a high degree of crystallinity (the average crystallite size is not less than 40 nm), without impure readily soluble magnesium phases (first of all, magnesium hydroxide) to obtain a homogeneous compound based on MPP matrix with a high compressive strength (up to 15 MPa). The specific surface of the conditioned MgO powder was no higher than 7 m^2/g [1]. It was also noted that the impurities in MgO of metal compounds, primarily silicon, calcium, and iron, do not significantly influence the synthesis conditions and the mechanical strength of the compound.

This article presents the results of studying the characteristics of MgO powder obtained from serpentinite, as well as determination of composition, mechanical strength, and hydrolytic stability of the prepared MPP matrix samples.

2. Materials and Methods

2.1. Obtaining MgO from Serpentinite

The flow chart for obtaining MgO from serpentinite is presented in Figure 1. In this work, an average sample of serpentinite from the "Bedenskoye" deposit, having a composition presented in Table 1, was used as a source of magnesium oxide.
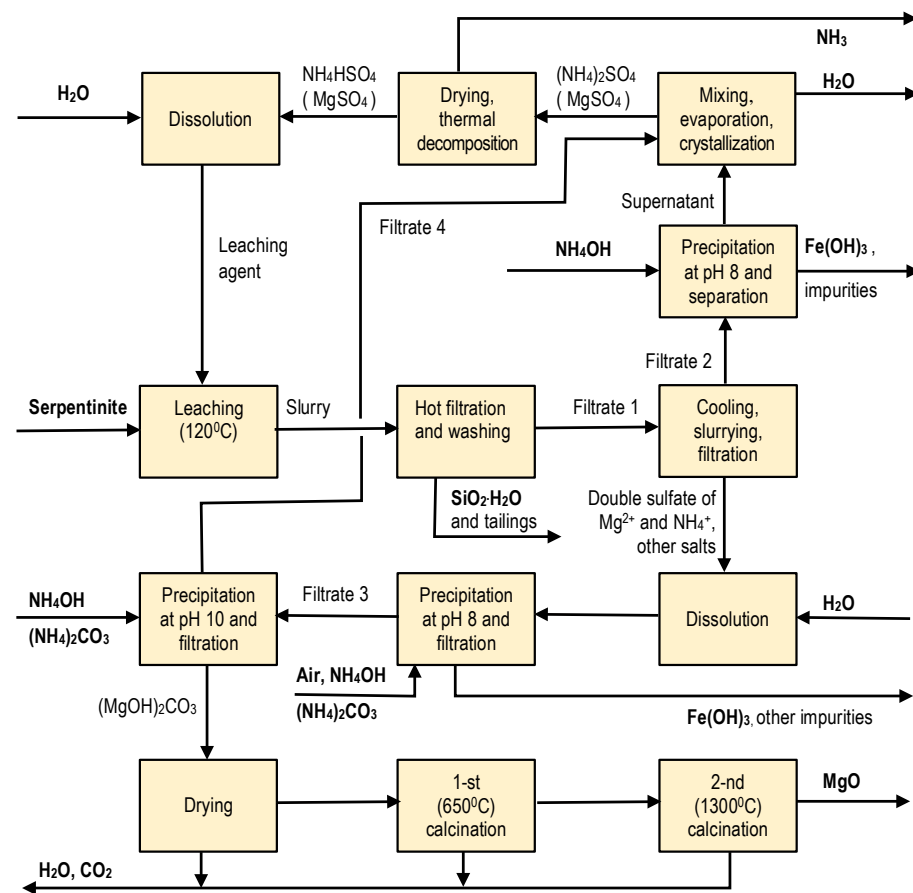
Figure 1. Flow chart for obtaining MgO from serpentinite.

Table 1. Chemical composition of serpentinite.

Content	MgO	SiO$_2$	Fe$_3$O$_4$	CaO	NiO	Al$_2$O$_3$	Cr$_2$O$_3$	MnO	SO$_3$	K$_2$O	Na$_2$O	LOI *
(wt%)	38.05	39.96	8.55	0.63	0.36	0.33	0.32	0.11	0.06	0.02	0.01	11.30

* Loss on Ignition.

Several repeated experiments were carried out to decompose serpentinite and remove magnesium hydroxide. In each of them, 100 g of finely ground serpentinite powder (with a grain boundary size d < 45 μm), obtained in a ball mill with ceramic balls, were placed in a laboratory autoclave with a mechanical stirrer, and 650 g (520 mL) of circulating solution containing 35% NaHSO$_4$, up to 7% MgSO$_4$ and up to 10% (NH$_4$)$_2$SO$_4$ were added. The mixture was stirred for 4 h at 120 °C. The obtained hot suspension was filtered under reduced pressure created by a water-jet pump on a Buchner filter with a thermostatic shirt at 95 °C to obtain filtrate No. 1, and then at the same temperature, the filter precipitate was washed by 250 mL of hot deionized water. Filtrate No. 1 and wash water were combined, and 912–925 g (730–740 mL) of mixed solution, containing no less than 3.4% of Mg(II) and no more than 0.08% of Fe(II, III), were obtained in different experiments that corresponded to the degree of magnesium removal—no less than 80%, and iron—up to 11.5%. The solution was placed in a cold-storage, where it was cooled to +4 °C and kept there for 2 h. As a result, a suspension was obtained, which was filtered on a thermostatted Buechner filter at 5 °C. Filtrate No. 2 (no more than 490 g with up to 0.5% magnesium and 0.1% iron) and a glassy precipitate with a pale yellowish-pink color were obtained. Chemical analysis of such precipitate (no less than 370 g), dried at 105 °C for 1 h until the loss of more than 10% moisture, showed a magnesium content of 6.5% and a molar ratio of Mg^{2+}:NH$_4^+$:SO$_4^{2-}$ = 1:2:2 that corresponded to the double salt—magnesium ammonium sulfate (Boussingaultite). The iron content in the dry sediment did not exceed 0.06%.

The precipitate was dissolved in 650 mL of hot deionized water (95 °C), and a 25% ammonia solution (purity qualification "analytical grade") was added to the obtained solution up to pH of 8, and 2 g of ammonium carbonate, $(NH_4)_2CO_3$ ("reagent grade"), was also added. A hot suspension of light green color was obtained, which was placed in an autoclave, in which the temperature was maintained at 95 °C. Air was passed through the suspension, adjusting the outlet of gases from the autoclave so that an excess pressure is created in it. The mixture was kept for 4 h with stirring. A light brown suspension was discharged from the autoclave, which was filtered through hot thermostatted Buchner filter with a water-jet pump using a filter with pore size 1–2.5 nm. The resulting filtrate No. 3 was again placed in an autoclave, previously washed with deionized water, and then filtrate No. 3 was cooled to room temperature. 80 mL of the solution of 25% ammonia were poured into the contents of the autoclave, and 45 g of ammonium carbonate were added. The autoclave was closed, the temperature was raised up to 65 °C, and the mixture was stirred under excess pressure for 4 h. A suspension of white color with a bluish sheen was obtained, which was filtered through a thermostatted Buchner filter using a paper filter with pore size 1–2.5 nm. Filtrate No. 4 and precipitate of magnesium hydroxide-carbonate were obtained. The precipitate was dried at 120 °C and then subjected to preliminary calcination at a temperature of 650 °C for 3 h.

Filtrate No. 2 was heated up to 50 °C, a 25% ammonia solution was added to it to pH 8, and the mixture was stirred for 5 h on a magnetic stirrer with heating. A finely dispersed light brown suspension was formed, which was separated in a laboratory centrifuge to obtain a supernatant.

The supernatant and filtrate No. 4 were mixed, and the resulting solution was subjected to vacuum evaporation on a Buchi R-124 rotary evaporator (Bunker Lake Blvd., Ramsey, MN, USA) at 85 °C and a pressure of 0.15 bar until a wet crystalline mass was obtained. This mass was placed in a muffle furnace and first dried at 120 °C for 1 h; then the temperature was raised to 310 °C and decomposition was carried out for another 7 h. In repeated experiments, at least 335 g of precipitate were obtained, to which 320 mL of deionized water and 5 g of ammonium sulfate were added after cooling. A recycled solution was obtained with a content of at least 35% $NaHSO_4$, up to 7% $MgSO_4$, and up to 10% $(NH_4)_2SO_4$, which was used to decompose the next portion of serpentinite.

In each of the consecutive carried out experiments, at least 30 g of the preproduct was obtained. The samples of magnesium oxide obtained in the course of six successive experiments were combined, and an average composition of precalcined magnesium oxide was obtained, in which the content of iron and manganese oxides did not exceed 0.01 wt%.

2.2. Preparation of the MPP Matrix

The synthesis of the MPP matrix was carried out according to reaction (1) at the MgO: H_2O:KH_2PO_4 weight ratio of 1:2:3. Previously in studies [1,13–16], it was shown that to reduce the rate of reaction (1) and, accordingly, to ensure a technologically acceptable setting time of the mixture for the purpose of high-quality mixing and tight packing of the resulting mixture into containers for subsequent storage, MgO powder should be used after preliminary heat treatment at 1300–1500 °C. Thus, MgO obtained from serpentinite in accordance with the method in Section 2.1 and precalcined at temperatures of 1300 °C for 3 h (hereinafter referred to as calcined MgO) in a muffle furnace (SNOL 30/1300, AB UMEGA GROUP, Utena, Lithuania) and KH_2PO_4 ("Rushim" LLC, Moscow, Russia) crushed to a particle size of 0.15–0.25 mm were used for synthesis of MPP matrix. The excess of MgO in relation to the stoichiometry of reaction (1) was 10 wt% [1]. To decrease the rate of reaction (1), boric acid was added to the initial mixture in an amount corresponding to its 1.5 wt% content in the sample. The obtained mixture was placed in PTFE molds.

Cubic samples of the MPP matrix with dimensions of $2 \times 2 \times 2$ cm^3 were prepared and kept for at least 15 days to cure at ambient atmospheric conditions.

2.3. Investigation of MgO and MPP Matrix Samples

The phase composition of MgO and MPP matrix samples was determined by X-ray diffraction (XRD) method using an Ultima-IV X-ray diffractometer (Rigaku, Tokyo, Japan). The XRD data were interpreted using the Jade 6.5 software package (MDI, Livermore, CA, USA) with PDF-2 powder database. The average crystallite size of the studied MgO samples was calculated by the Scherrer [12]. The composition of MgO was determined using the Rietveld method [17], with a PROFEX GUI software package for BGMN [18].

The microstructure of MgO and MPP matrix samples was investigated by the scanning electron microscopy (SEM) using a JSM-6700F (Jeol, Tokyo, Japan) and Vega 3 (Tescan, Brno, Czech Republic) microscopes; the electron probe microanalysis of the samples was performed by energy-dispersive X-ray spectroscopy (EDS) using an X-ACT analyzer (Oxford Inst., High Wycombe, UK).

The elemental composition of MgO powder was studied using an Axious Advanced PW 4400/04 X-ray fluorescence (XRF) spectrometer (PANalytical B.V., Almelo, Netherlands).

Adsorption measurements of MgO powder samples were carried out in an ASAP 2000 automatic sorbtometer (Micromeritics, Norcross, GA, USA); the specific surface area was calculated using the Micromeritics software package.

The particle size distribution of MgO samples was determined using a SALD-7500 nano laser diffraction granulometer (Shimadzu, Kyoto, Japan), including the use of 60 W ultrasound for 5 min.

The compressive strength of MPP matrix samples was determined using a Cybertronic 500/50 kN test machine (Testing Bluhm & Feuerherdt GmbH, Germany). At least three compound samples were used in experiment.

The hydrolytic stability of MPP matrix samples was determined in accordance with the semi-dynamic standard test GOST R 52126-2003 [19]. Before leaching, monolithic cubic samples were immersed in ethanol for 5–7 s, then the samples were dried in air for 30 min. Next, the samples were placed in a PTFE container, and double-distilled water was poured in as a leaching agent (pH 6.6 ± 0.1, volume 100 mL), which was replaced at regular time intervals. The samples were removed from the container at the set time, washed with double-distilled water (volume 100 mL), and combined with the leachate, and the content of the matrix components in the solutions after leaching was determined by ICP–AES (iCAP-6500 Duo, Thermo Scientific, Waltham, MA, USA). The calculations of the differential leaching rate LR_{dif} (g/(cm²·day)) of the matrix components from samples were made according to Equation (2).

$$LR = \frac{c \cdot V}{S \cdot f \cdot t},\qquad(2)$$

where c—element concentration in solution after leaching, g/L; V—the volume of leaching agent, L; S—the open geometric surface area of the monolithic samples, cm²; f—element content in matrix, g/g; and t—leaching time, days (for calculating the differential leaching rate t—duration of the n-th leaching period between shifts of contact solution).

Leaching mechanism of MPP matrix components was assessed according to a de Groot and van der Sloot model [20], which can be presented as Equation (3), where values of the coefficient A (slope of the line) correspond to the following mechanisms: <0.35—surface wash-off (or a depletion if it is found in the middle or at the end of the test); 0.35–0.65—diffusion transport; and >0.65—surface dissolution [21]. The calculation of B_i was carried out according to Equation (4).
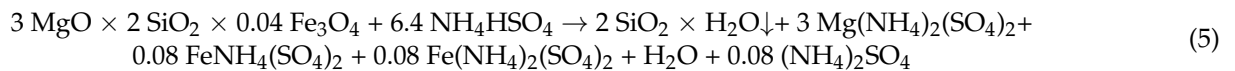
$$\log(B_i) = A \log(t_n) + const\qquad(3)$$

$$B_i = A_n \cdot \frac{V}{S} \cdot \frac{\sqrt{t_n}}{\left(\sqrt{t_n} - \sqrt{t_{n-1}}\right)}\qquad(4)$$

3. Results and Discussion

3.1. Features of the Obtaining Process of MgO from Serpentinite
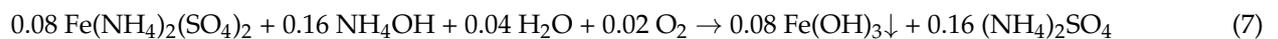
The advantage of the bisulfate method of serpentinite reprocessing provides the possibility of creating a closed-loop technological process, where all reagents are recovered. This process was first proposed in [22]. In contrast to the complex chemical formulas used in this work, we introduced simplifications that make it possible to better understand the discussed cyclic process. If we present the formula of serpentinite in the form of a ratio of the main macrocomponents, oxides of magnesium, silicon, and iron, in accordance with the composition presented in Table 1, then the process of decomposition of serpentinite with ammonium bisulfate can be presented as reaction (5).

$$3\,MgO \times 2\,SiO_2 \times 0.04\,Fe_3O_4 + 6.4\,NH_4HSO_4 \rightarrow 2\,SiO_2 \times H_2O\downarrow + 3\,Mg(NH_4)_2(SO_4)_2 + \\ 0.08\,FeNH_4(SO_4)_2 + 0.08\,Fe(NH_4)_2(SO_4)_2 + H_2O + 0.08\,(NH_4)_2SO_4 \tag{5}$$

In reaction (5), in contrast to [22], it was taken into account that in concentrated solutions containing sulfate and ammonium, Mg (II) sulfate and Fe (II) and Fe (III) sulfates form double salts with ammonium sulfate [23,24]. From the mixture obtained in accordance with reaction (5), it is possible to separate the silicic acid phase (as well as the undecomposed part of serpentinite, which takes place under the usually used real conditions), but this separation is possible only at elevated temperature, since the solubility of double magnesium sulfate and ammonium decreases sharply with temperature decreasing. Therefore, the separation in the work presented by us is carried out at temperatures above 90 °C. In this case, a simple cooling operation allows most of the magnesium to be removed from the system in the form of Boussingaultite, reaction (6).

$$3\,Mg(NH_4)_2(SO_4)_2 + 18\,H_2O \rightarrow 3\,Mg(NH_4)_2(SO_4)_2 \times 6H_2O\downarrow \tag{6}$$
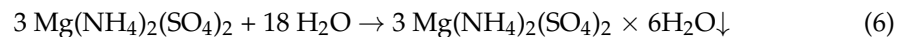
This process, similar to recrystallization, significantly reduces the problems of further purification of the magnesium product. However, it should be taken into account that all Tutton salts (double sulfates formed by two and singly charged cations) with a monoclinic crystal structure are capable of cocrystallization; therefore, Mohr's salt Fe ($Fe(NH_4)_2(SO_4)_2 \times 6H_2O$), like a similar manganese salt, can pollute the Boussingaultite. That is why at the stage of purification of a magnesium compound not an ammonia solution is used, but a mixture of an ammonia solution and ammonium carbonate, since it is impossible to achieve quantitative precipitation of manganese hydroxide at pH 8. Within the framework of the processes presented for macrocomponents, the purification of double magnesium and ammonium sulfate from iron occurs in the following simple way, reaction (7).

$$0.08\,Fe(NH_4)_2(SO_4)_2 + 0.16\,NH_4OH + 0.04\,H_2O + 0.02\,O_2 \rightarrow 0.08\,Fe(OH)_3\downarrow + 0.16\,(NH_4)_2SO_4 \tag{7}$$

The Fe (III) double salt (ferric ammonium alum) predominantly remains in the filtrate after the Boussingaultite is separated. The filtrate is purified from iron by the reaction (8).

$$0.08\,FeNH_4(SO_4)_2 + 0.24\,NH_4OH \rightarrow 0.08\,Fe(OH)_3\downarrow + 0.16\,(NH_4)_2SO_4 \tag{8}$$

A very important problem is the problem of magnesium precipitation from double ammonium magnesium sulfate. Magnesium hydroxide is practically impossible to quantitatively precipitate with just ammonia from solutions containing excessive amounts of ammonium sulfate. We used the process of precipitation of a hydroxide-carbonate complex, similar to the analogous process in [22], according to reaction (9).

$$3\,Mg(NH_4)_2(SO_4)_2 + 3\,NH_4OH + 1.5\,(NH_4)_2CO_3 \rightarrow 1.5\,(MgOH)_2CO_3\downarrow + 6\,(NH_4)_2SO_4 \tag{9}$$
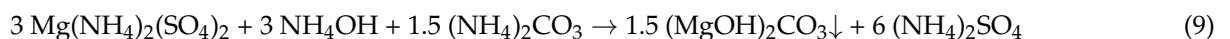
Reactions (5), (7)–(9) give a total of 6.4 mol of ammonium sulfate. Removal in solid form by evaporation and subsequent heat treatment of ammonium sulfate leads to the production of all reagents necessary for the implementation of the cyclic process, reaction (10).

$$6.4\ (NH_4)_2SO_4 \rightarrow 6.4\ NH_4HSO_4 + 6.4\ NH_3 \qquad (10)$$
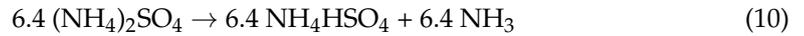
In particular, when this amount of ammonia is dissolved, 6.4 mol of its aqueous solution can be obtained, of which 3.4 mol isfor carrying out reactions (7)–(9), as well as 3 mol for obtaining 1.5 mol of $(NH_4)_2CO_3$ for reaction (9). A real technological process can also be closed in terms of carbon dioxide, which is released during the calcination of magnesium hydroxide-carbonate obtained in accordance with reaction (9).

While carrying out sequentially repeated laboratory experiments, as can be seen from the description in Section 2.1, a closed process for ammonium bisulfate was carried out. To standardize the conditions for laboratory experiments, the collection of gas components and recuperation of ammonia solution on a small scale were not carried out.

According to our estimates, the cost of the enlarged proposed process for the production of MgO from serpentinite should not exceed $400 per ton, which corresponds to the cost of Portland cement.

3.2. Effect of Calcination of MgO Powder

The obtained X-ray diffraction patterns of MgO powder samples are shown in Figure 2. It was established that the dominant phase in the studied samples is the target phase with the periclase structure, which is identified by the reflexes 2.43, 2.11, and 1.49 Å (Figure 2). The average crystallite size of MgO and calcined MgO was 40 and 62 nm, respectively, which corresponds to the requirements [12]. It should be noted that MgO samples prepared by high-temperature processing do not contain an impurity (Figure 2b) of $Mg(OH)_2$ (brucite) and $Mg_5(CO_3)_4(OH)_2 \times 4H_2O$ (hydromagnesite), which present in amounts about 21 and about 7 wt%, respectively, in the initial MgO sample (Figure 2a). It was previously noted that the presence of such phases in MgO during the synthesis of the MPP matrix is extremely undesirable, because it leads to an unacceptable increase in the rate of reaction (1) and produces an inhomogeneous compound with low strength.
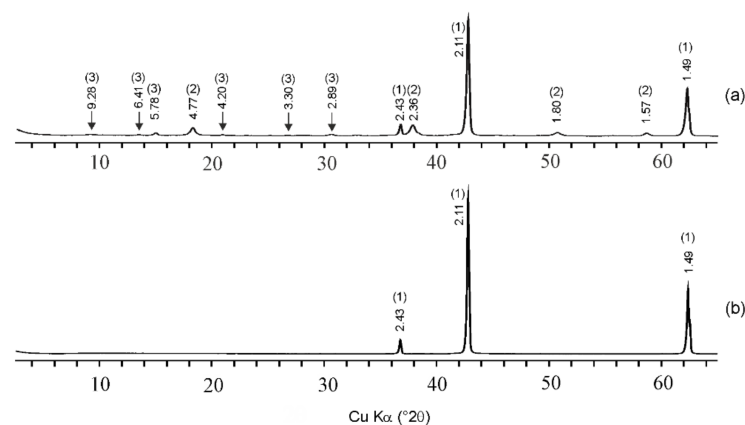

Figure 2. X-ray diffraction patterns of MgO (**a**) and calcined MgO (**b**). 1—MgO (periclase); 2—$Mg(OH)_2$ (brucite), 3—$Mg_5(CO_3)_4(OH)_2 \times 4H_2O$ (hydromagnesite).

According to XRF analysis, the calcined sample of magnesium oxide contains 0.22 wt% impurities (Table 2), that corresponds to the chemical purity of reagent "analytical grade" in accordance with Russian standard [25].

Table 2. Chemical composition of calcined MgO.

Component Content (wt%)	
MgO	**Impurities**
99.78	SiO_2—0.10; CaO—0.08; Fe_2O_3—0.01; MnO—0.02; P_2O_5—0.01

When studying the morphology of MgO powder particles, it was found that the initial sample consists of particles of irregular shape with a size of several to tens of μm (Figure 3a), and the surface structure of this powder presents staggered flake layer, which is typical of $Mg(OH)_2$ (Figure 3b). The morphology of MgO changed from a flake appearance into cubic crystals (Figure 3c) after its calcination; the discovered effect was previously also observed in [16].

(**a**)

(**b**)

(**c**)
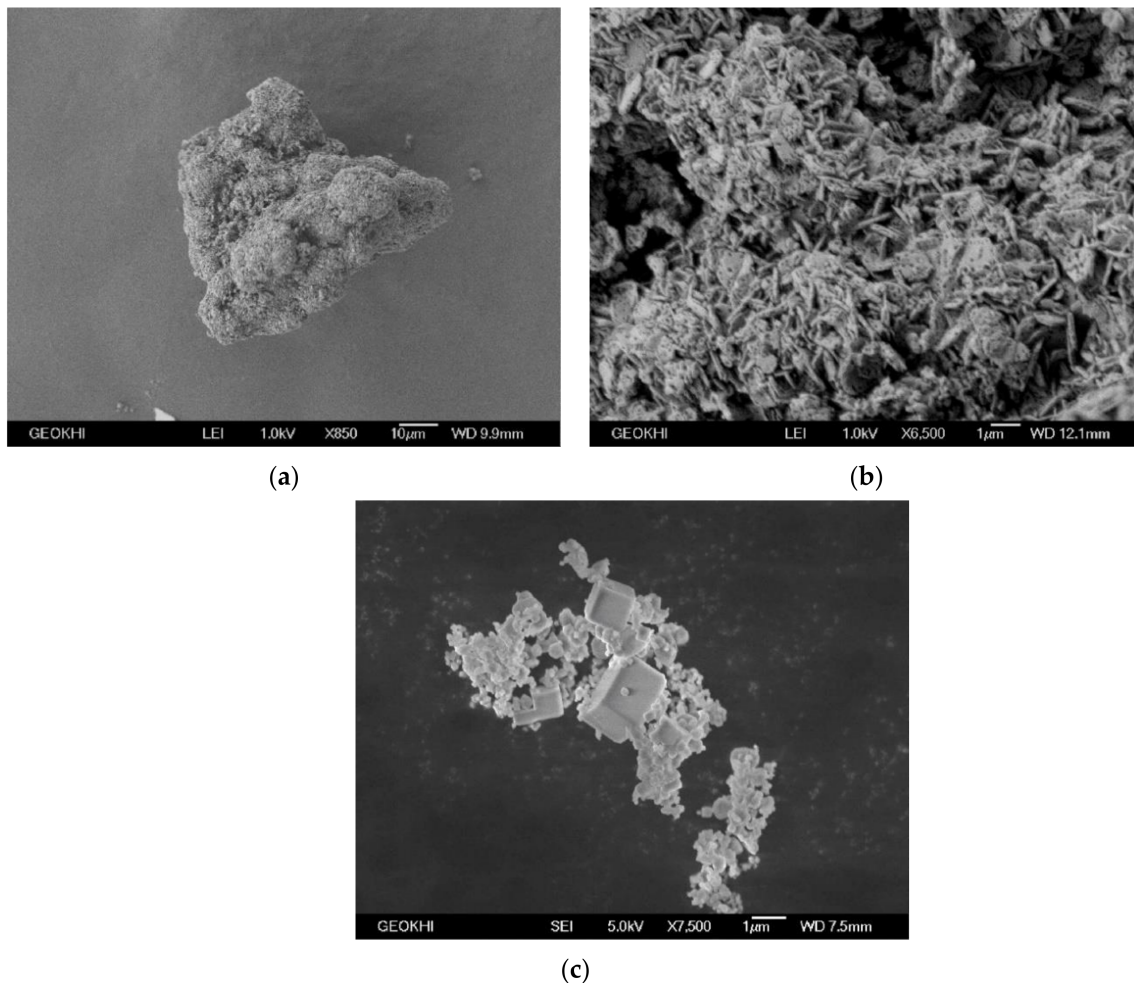
Figure 3. Scanning electron microscope (SEM) images of MgO (**a**,**b**) and calcined MgO (**c**).

The obtained data on the granulometric composition of MgO powders are presented in Figure 4 and in Table 3. The distribution of particle agglomerates by size of the initial and calcined powder can be characterized as monomodal with a value of about 55 μm and a complication in the region of small sizes with values less than 1 μm (Figure 4a) and less than 3 μm (Figure 4c), respectively. The effect of ultrasound on MgO samples leads to the destruction of large agglomerates. For example, as a result of the influence of ultrasound on the initial powder, about 56% of the particles acquire a size of less than 8 μm (Figure 4a,b), and in the case of a calcined powder, about 79%—less than 31 μm (Figure 4c,d). It is noted

that, in general, calcination leads to partial agglomeration of MgO particles, for example, to an increase of the number of aggregates with a size of about 100 μm (Figure 4d).
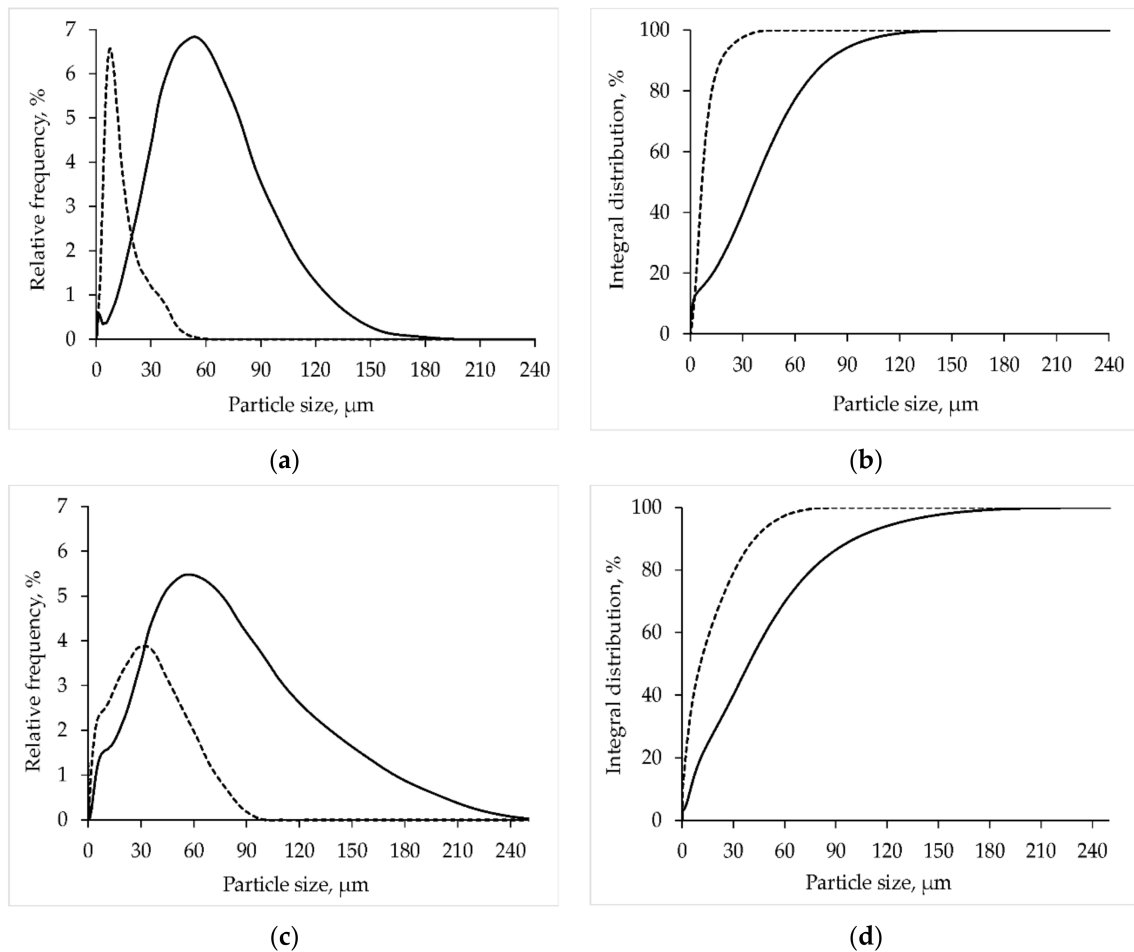

Figure 4. Size distribution of MgO (**a**,**b**) and calcined MgO (**c**,**d**) (dashed curve—size distribution after the effects of ultrasound on powders).

Table 3. The results of granulometric analysis of MgO.

Sample	Mode (μm)	Median (μm)	>90% (μm)	<0.1 μm	<1 μm	<10 μm	<100 m
MgO	54.92	37.09	87.51	0.99%	8.04%	18.20%	98.12%
Calcined MgO	54.92	38.92	110.47	0.71%	3.51%	19.77%	92.35%
MgO *	7.58	6.81	19.26	no	3.70%	74.13%	100%
Calcined MgO *	30.68	10.58	43.51	4.73%	14.64%	50.32%	100%

* After exposure by ultrasound on powders.

It was found that the initial MgO powder has a large specific surface area (64.5 m^2/g), apparently due to the flake layer structure. In this case, as a result of calcining MgO powder at 1300 °C for 3 h, the specific surface area of magnesium oxide decreases to 5.4 m^2/g, which corresponds to the previously obtained data [1].

3.3. Study of the Obtained Samples of the MPP Matrix

For the synthesis of the MPP matrix, we used a precalcined MgO powder, the characteristics of which are given in the previous Section. When studying the phase composition of the synthesized samples of the MPP matrix, it was found that their main crystalline

phase is the target phase $MgKPO_4 \times 6H_2O$, which is an analog of K-struvite [6] with main reflections at 5.86; 5.56; 5.40; 4.25; 4.13 Å etc.) (Figure 5). The samples also contain phase of MgO (periclase), which is associated with the excess of the used MgO in relation to the stoichiometry of reaction (1).
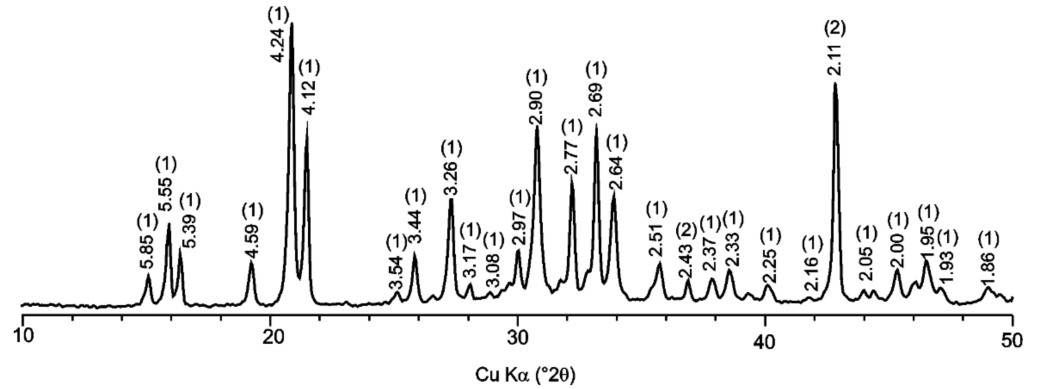

Figure 5. X-ray diffraction pattern of the magnesium potassium phosphate (MPP) matrix. 1—$MgKPO_4 \times 6H_2O$ (K-struvite); 2—MgO (periclase).

The SEM micrograph of the surface of the MPP compound is shown in Figure 5. The elemental composition of the predominant phases in the compound sample includes matrix components of the basic composition $MgKPO_4 \times 6H_2O$ with insignificant variations in the Mg/K ratio, as we noted earlier in [1]. Open pores with a linear size of about 100 μm are also observed (Figure 6).


Figure 6. SEM image of the MPP matrix.

The compressive strength of the MPP matrix obtained using MgO after calcining at 1300 °C for 3 h was 6.19 ± 0.45 MPa, which meets the regulatory requirements for a cement compound: no less than 4.9 MPa [26].

The determination results of hydrolytic stability of MPP compound to the leaching of matrix-forming components are shown in Figure 7a,b. Data in Figure 7a shows that the differential leaching rate of magnesium, potassium, and phosphorus from the compound on the 91st day of contact of the sample with water is 1.6×10^{-5}, 4.7×10^{-4} и8.9×10^{-5} g/(cm^2 day),

respectively. It was found that the leaching of the matrix-forming elements for 91 days of contact of the sample with water is controlled by various mechanisms. Leaching of potassium and phosphorus from the MPP matrix in the first seven days occurs due to its wash-off of from the surface of the compound, followed by depletion of the surface layer (Figure 7b, coefficients A in Equation (3) are for potassium −0.43 and 0.17, and for phosphorus −0.50, 0.04, and −0.66). Leaching of magnesium in the first 10 days occurs due to its wash-off of from the surface of the compound, and in the next 81 days due to diffusion from its inner layers (Figure 7b, −0.81 and 0.48). The obtained results on the hydrolytic stability (rate and mechanism of leaching) of the MPP matrix obtained using MgO obtained from serpentinite are consistent with the previously obtained data for the MPP matrix obtained from commercial MgO [1].
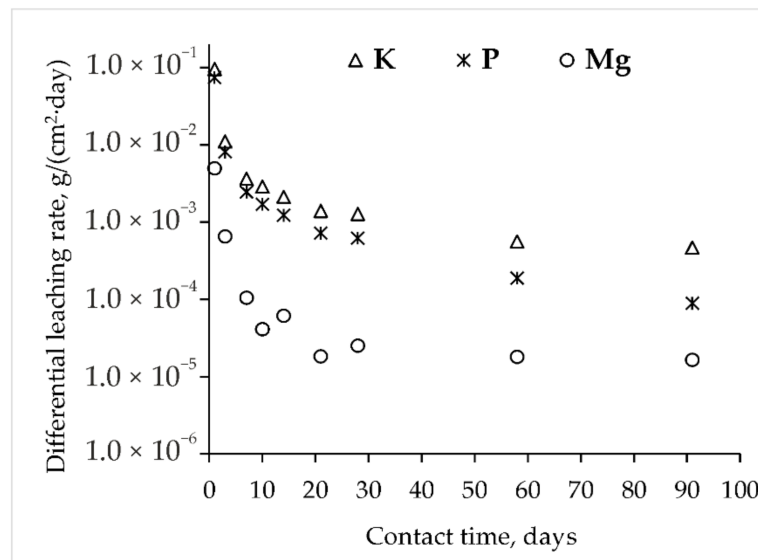
(a)
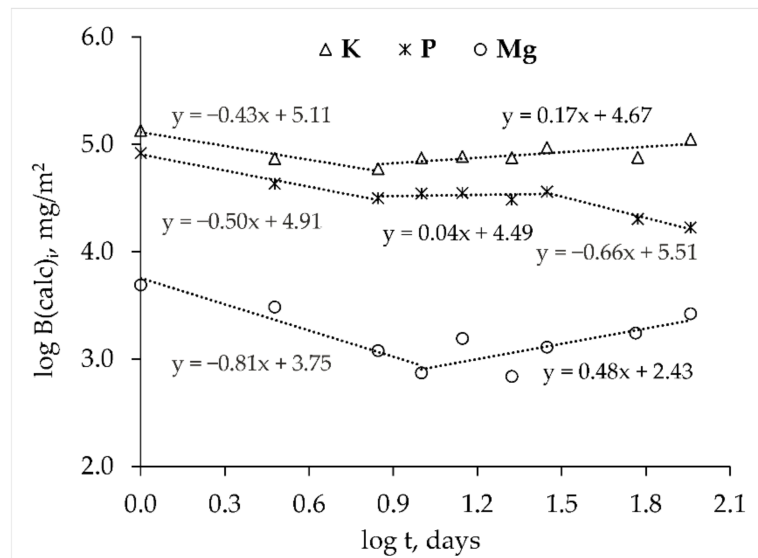
(b)

Figure 7. Kinetic curve of the leaching rate (**a**) and logarithmic dependence of the release (**b**) of the matrix components from the MPP matrix.

4. Conclusions

The applicability of MgO obtained during the reprocessing of widely available mineral raw materials—serpentinite by almost waste-free and economically profitable way for the

synthesis of the MPP matrix was established. The characteristics of the obtained matrix correspond to the requirements for the material for RW immobilization and for preventing of release of highly toxic radionuclides into the environment.

References

1. Vinokurov, S.E.; Kulikova, S.A.; Krupskaya, V.V.; Myasoedov, B.F. Magnesium potassium phosphate compound for radioactive waste immobilization: Phase composition, structure, and physicochemical and hydrolytic durability. *Radiochemistry* **2018**, *60*, 70–78. [CrossRef]
2. Vinokurov, S.E.; Kulikova, S.A.; Myasoedov, B.F. Solidification of high level waste using magnesium potassium phosphate compound. *Nucl. Eng. Technol.* **2019**, *51*, 755–760. [CrossRef]
3. Kulikova, S.A.; Vinokurov, S.E. The influence of zeolite (Sokyrnytsya deposit) on the physical and chemical resistance of a magnesium potassium phosphate compound for the immobilization of high-level waste. *Molecules* **2019**, *24*, 3421. [CrossRef] [PubMed]
4. Dmitrieva, A.V.; Kalenova, M.Y.; Kulikova, S.A.; Kuznetsov, I.V.; Koshcheev, A.M.; Vinokurov, S.E. Magnesium-potassium phosphate matrix for immobilization of ^{14}C. *Russ. J. Appl. Chem.* **2018**, *91*, 641–646. [CrossRef]
5. Kulikova, S.A.; Belova, K.Y.; Tyupina, E.A.; Vinokurov, S.E. Conditioning of spent electrolyte surrogate LiCl-KCl-CsCl using magnesium potassium phosphate compound. *Energies* **2020**, *13*, 1963. [CrossRef]
6. Graeser, S.; Postl, W.; Bojar, H.-P.; Berlepsch, P.; Armbruster, T.; Raber, T.; Ettinger, K.; Walter, F. Struvite-(K), $KMgPO_4 \cdot 6H_2O$, the potassium equivalent of struvite—A new mineral. *Eur. J. Miner.* **2008**, *20*, 629–633. [CrossRef]
7. Sasaki, K.; Moriyama, S. Effect of calcination temperature for magnesite on interaction of MgO-rich phases with boric acid. *Ceram. Int.* **2014**, *40*, 1651–1660. [CrossRef]
8. Yu, J.; Qian, J.; Wang, F.; Li, Z.; Jia, X. Preparation and properties of a magnesium phosphate cement with dolomite. *Cem. Concr. Res.* **2020**, *138*, 106235. [CrossRef]
9. Sirota, V.; Selemenev, V.; Kovaleva, M.; Pavlenko, I.; Mamunin, K.; Dokalov, V.; Yapryntsev, M. Preparation of crystalline $Mg(OH)_2$ nanopowder from serpentinite mineral. *Int. J. Min. Sci. Technol.* **2018**, *28*, 499–503. [CrossRef]
10. Zhao, Q.; Liu, C.-J.; Jiang, M.-F.; Saxén, H.; Zevenhoven, R. Preparation of magnesium hydroxide from serpentinite by sulfuric acid leaching for CO_2 mineral carbonation. *Miner. Eng.* **2015**, *79*, 116–124. [CrossRef]
11. Teir, S.; Kuusik, R.; Fogelholm, C.-J.; Zevenhoven, R. Production of magnesium carbonates from serpentinite for long-term storage of CO_2. *Int. J. Miner. Process.* **2007**, *85*, 1–15. [CrossRef]
12. Vinokurov, S.E.; Kulikova, S.A.; Krupskaya, V.V.; Tyupina, E.A. Effect of characteristics of magnesium oxide powder on composition and strength of magnesium potassium phosphate compound for solidifying radioactive waste. *Russ. J. Appl. Chem.* **2019**, *92*, 490–497. [CrossRef]
13. Wagh, A.S. *Chemically Bonded Phosphate Ceramics: Twenty-First Century Materials with Diverse Application*, 2nd ed.; Elsevier: Amsterdam, The Netherlands, 2016; pp. 1–422.
14. Tan, Y.; Yu, H.; Li, Y.; Wu, C.; Dong, J.; Wen, J. Magnesium potassium phosphate cement prepared by the byproduct of magnesium oxide after producing Li_2CO_3 from salt lakes. *Ceram. Int.* **2014**, *40*, 13543–13551. [CrossRef]

15. Viani, A.; Sotiriadis, K.; Šašek, P.; Appavou, M.-S. Evolution of microstructure and performance in magnesium potassium phosphate ceramics: Role of sintering temperature of MgO powder. *Ceram. Int.* **2016**, *42*, 16310–16316. [CrossRef]

16. Dong, J.; Yu, H.; Xiao, X.; Li, Y.; Wu, C.; Wen, J.; Tan, Y.; Chang, C.; Zheng, W. Effects of calcination temperature of boron-containing magnesium oxide raw materials on properties of magnesium phosphate cement as a biomaterial. *J. Wuhan Univ. Technol. Sci. Ed.* **2016**, *31*, 671–676. [CrossRef]

17. Post, J.E.; Bish, D.L. Rietveld refinement of crystal structures using powder X-ray diffraction data. In *Modern Powder Diffraction, Reviews in Mineralogy*; MSA: Washington, DC, USA, 1989; pp. 277–308.

18. Döbelin, N.; Kleeberg, R. Profex: A graphical user interface for the Rietveld refinement program BGMN. *J. Appl. Crystallogr.* **2015**, *48*, 1573–1580. [CrossRef] [PubMed]

19. Russian Federation. *Radioactive Waste. Long Time Leach Testing of Solidified Radioactive Waste Forms*; GOST R 52126-2003; Standard-inform: Moscow, Russia, 2003; pp. 1–8.

20. De Groot, G.; van der Sloot, H. Determination of leaching characteristics of waste materials leading to environmental product certification. In *Stabilization and Solidification of Hazardous, Radioactive, and Mixed Wastes*; Gilliam, T., Wiles, C., Eds.; ASTM International: West Conshohocken, PA, USA, 1992; Volume 2, pp. 149–170.

21. Torras, J.; Buj, I.; Rovira, M.; de Pablo, J. Semi-dynamic leaching tests of nickel containing wastes stabilized/solidified with magnesium potassium phosphate cements. *J. Hazard. Mater.* **2011**, *186*, 1954–1960. [CrossRef] [PubMed]

22. Pundsack, F.L. Recovery of Silica, Iron Oxide and Magnesium Carbonate from the Treatment of Serpentine with Ammonium Bisulfate. U.S. Patent 3,338,667, 29 August 1967.

23. Khamizov, R.K.; Zaitsev, V.A.; Gruzdeva, A.N.; Krachak, A.N.; Rarova, I.G.; Vlasovskikh, N.S.; Moroshkina, L.P. Feasibility of acid–salt processing of alumina-containing raw materials in a closed-loop process. *Russ. J. Appl. Chem.* **2020**, *93*, 1059–1067. [CrossRef]

24. Nduagu, E.; Highfield, J.; Chen, J.; Zevenhoven, R. Mechanisms of serpentine–ammonium sulfate reactions: Towards higher efficiencies in flux recovery and Mg extraction for CO_2 mineral sequestration. *RSC Adv.* **2014**, *4*, 64494–64505. [CrossRef]

25. Russian Federation. *Reagents. Magnesium oxide. Specifications*; GOST 4526-75; Standardinform: Moscow, Russia, 1975; pp. 1–11.

26. Russian Federation. Collection, processing, storage and conditioning of liquid radioactive waste. Safety requirements. In *Federal Norms and Rules in the Field of Atomic Energy Use*; NP-019-15; Rostekhnadzor: Moscow, Russia, 2015; pp. 1–22.